





Fronto-cerebellar connectivity disruptions and functional reorganization in Friedreich's Ataxia: A structural and resting-state fMRI study

Ravi Dadsena^{a,b} , Sandro Romanzetti^{a,b}, Stella Andrea Lischewski^a, Yinghua Jing^a, Dagmar Timmann^c, Jennifer Faber^{d,e}, Jörg B. Schulz^{a,b}, Kathrin Reetz^{a,b,*} , Imis Dogan^{a,b}, on behalf of the FACROSS study group

^a Department of Neurology, RWTH Aachen University 52074, Aachen, Germany

^b JARA Brain Institute Molecular Neuroscience and Neuroimaging (INM-11), Research Centre Jülich and RWTH Aachen University 52056, Aachen, Germany

^c Department of Neurology and Center for Translational Neuro- and Behavioral Sciences (C-TNBS), Essen University Hospital, University of Duisburg-Essen 45147, Essen, Germany

^d German Center for Neurodegenerative Diseases (DZNE) 53127, Bonn, Germany

^e Department of Neurology, University Hospital Bonn 53127, Bonn, Germany

ARTICLE INFO

Keywords:

Friedreich's ataxia
Resting-state fMRI
Structural MRI
Cross-sectional study
Neuroimaging
Brain connectivity
Clinical correlations

ABSTRACT

Friedreich's ataxia (FRDA) is an inherited neurodegenerative disorder characterized by progressive ataxia and multisystem manifestations resulting from involvement of the peripheral and central nervous systems. While regional atrophy is known to be associated with symptoms, functional network alterations may represent a critical pathological mechanism; however, their specific contribution to motor and cognitive impairment remains unclear. We combined T1-weighted anatomical MRI and resting-state functional MRI (rs-fMRI) in 37 individuals with FRDA and 41 age- and sex-matched healthy controls and explored how functional connectivity differences are related to atrophy, clinical severity and cognitive performance. Regional volumes were quantified using morphometry analyses, spontaneous rs-fMRI activity was assessed via amplitudes of low-frequency fluctuations, and functional co-activation was evaluated among regions showing structural and neuronal activity alterations. Volume reductions were most pronounced in the brainstem, cerebellar white matter, hemisphere of lobules VI, X, and thalamus. Functionally, individuals with FRDA showed decreased fronto-cerebellar connectivity alongside increased intracerebellar, thalamo-striatal, and hippocampal-cerebellar coupling. Infratentorial and thalamic volume loss correlated strongly with clinical disease severity, whereas reduced frontal co-activation with cerebellar lobules VI, Crus I and II was moderately associated with poorer motor and cognitive performance. In contrast, increased intracerebellar and hippocampal-cerebellar coupling was observed particularly in individuals with more advanced disease and was partly associated with better cognitive outcomes. These findings indicate widespread disruptions of long-range cerebro-cerebellar connectivity together with increased intraregional coupling and potential network reorganization, underscoring the importance of network-level mechanisms for understanding clinical heterogeneity in FRDA and guiding future prognostic and therapeutic studies.

1. Introduction

Friedreich's ataxia (FRDA) is a rare neurodegenerative disorder with typical onset in childhood or adolescence, leading to progressive motor dysfunction, loss of coordination, and a range of systemic manifestations, including hypertrophic cardiomyopathy, musculoskeletal deformities and metabolic dysfunction (Reetz et al., 2025, 2018). Genetically, FRDA is most frequently caused by a homozygous GAA

triplet repeat expansion within the *FXN* gene, resulting in deficient production of the mitochondrial protein frataxin (Campuzano et al., 1996). The subsequent mitochondrial dysfunction and oxidative stress primarily damage the nervous system, targeting the dorsal root ganglia, spinocerebellar tracts, and cerebellum (Koeppen and Mazurkiewicz, 2013). Despite advances in our understanding of FRDA in recent years, the pathophysiological mechanisms underlying neurodegeneration and the heterogeneous phenotype remain complex and poorly elucidated.

* Corresponding author at: Department of Neurology, Pauwelsstraße 30, 52074 Aachen, Germany.

E-mail address: kreetz@ukaachen.de (K. Reetz).

<https://doi.org/10.1016/j.neuroimage.2026.121872>

Received 14 January 2026; Received in revised form 26 February 2026; Accepted 20 March 2026

Available online 20 March 2026

1053-8119/© 2026 The Authors. Published by Elsevier Inc. This is an open access article under the CC BY license (<http://creativecommons.org/licenses/by/4.0/>).

Continued research, particularly through advanced neuroimaging studies, is needed to better bridge the gap between neuropathological changes and clinical manifestations.

Structural neuroimaging studies using magnetic resonance imaging (MRI) have provided insights into the neuroanatomical alterations in FRDA, most prominently in the spinal cord, brainstem, and cerebellar regions correlating with disease progression and ataxia severity (Adanyeguh et al., 2023; Dogan et al., 2019; Rezende et al., 2023; Selvadurai et al., 2021). Recent large-scale investigations, including the first cross-sectional findings of the global TRACK-FA study and retrospective multinational MRI data aggregation of the ENIGMA-Ataxia Working Group, demonstrated large effect-sizes of volumetric reductions in the dentate nucleus, cerebellar peduncles and brainstem as early features of the disease, whereas cerebellar and cerebral gray matter loss evolve at later stages (Georgiou-Karistianis et al., 2025; Harding et al., 2021). Diffusion tensor imaging studies have reported microstructural white matter alterations in corticospinal tracts and cerebro-cerebellar pathways (Adanyeguh et al., 2023; Della Nave et al., 2008; Kerestes et al., 2023; Selvadurai et al., 2020). Importantly, however, structural change alone cannot fully explain the clinical variability of FRDA, and emerging evidence indicates widespread functional network alterations that may contribute to symptom heterogeneity (Vavla et al., 2022). Alongside structural connectivity measures, functional MRI (fMRI) is therefore essential to elucidate how neurodegeneration alters cerebello-cerebral network integrity and to potentially identify adaptive functional reorganization patterns. Moreover, functional imaging enables the detection of network-level dysfunction that can precede overt and irreversible atrophy, thereby offering deeper insight into disease progression and informing the development of targeted therapeutic interventions (Hohenfeld et al., 2018).

In FRDA, task-based fMRI studies employing motor or nonmotor tasks have shown a mixed pattern of hypoactivation and hyperactivation in cerebral and cerebellar regions, as well as reduced cerebello-cerebral functional connectivity (Dogan et al., 2016; Harding et al., 2015; Vavla et al., 2022). Resting-state functional MRI (rs-fMRI) offers a valuable perspective by enabling the investigation of the brain's intrinsic connectivity patterns in the absence of explicit tasks. However, only few studies utilized rs-fMRI in FRDA and revealed altered cerebello-cortical and intra-cerebellar connectivity, which are thought to reflect a loss of neural synchronization and network efficiency contributing to the clinical presentation of the disease (Cocozza et al., 2018; Kerestes et al., 2023; Tranfa et al., 2025). Reduced connectivity between the cerebellum and motor cortex was also shown to correlate with motor performance and white matter integrity in cerebellar pathways (Kerestes et al., 2023). While such findings highlight the potential of rs-fMRI to explore functional network disruptions in motor and sensory circuits, our understanding of how neuroanatomical and neurofunctional alterations interact and contribute to disease progression remains insufficiently characterized.

In this paper, we aim to bridge critical gaps in our understanding of FRDA by employing both structural and functional neuroimaging and investigate how regional volume loss, clinical symptoms and cognitive performance are linked to functional connectivity alterations. We use voxelwise measures, including amplitude of low-frequency fluctuations (ALFF) and fractional ALFF (fALFF), to assess spontaneous neural activity in individuals with FRDA compared to healthy controls. Brain regions showing alterations in intrinsic activity alongside structurally affected areas are used as region-of-interest (ROI)-based functional connectivity analyses to evaluate inter-regional communication. These complementary approaches of both anatomical and functional imaging provide an integrated view of network dysfunction in FRDA and are essential to capture the interplay between structural degeneration and network dysfunction. Ultimately, our findings provide insights into altered cerebello-cerebral and intracerebellar network dynamics that could inform the development of reliable imaging markers for disease

monitoring and therapeutic evaluation and potentially pave the way for more targeted treatment strategies.

2. Methods

2.1. Study participants

This study was conducted as part of the European Friedreich's Ataxia Consortium for Translational Studies (EFACTS) (Reetz et al., 2021, 2016, 2015) at the University Hospital RWTH Aachen, Germany. Participants were asked to participate in an MRI sub-study, which was approved by the local ethics committee (EK083/15, EK057/10), in accordance with the Declaration of Helsinki. Written informed consent was obtained from all participants prior to their inclusion in the study, ensuring ethical conduct and full participant awareness throughout the research. A total of 37 adult individuals with genetically confirmed FRDA were recruited and compared to 41 healthy control participants without any history of neurological or psychiatric disorders. Participants were eligible if they were aged 18 years or older. Exclusion criteria for MRI included any contraindications, such as metallic implants or claustrophobia.

2.2. Clinical and neuropsychological assessments

Clinical evaluations included the Scale for the Assessment and Rating of Ataxia (SARA) to quantify ataxia severity (Schmitz-Hübbsch et al., 2006), the Activities of Daily Living (ADL) Scale to assess functional impairment, and the Inventory of Non-Ataxia Signs (INAS) to capture non-ataxia symptoms and signs such as paresis and sensory deficits (Jacobi et al., 2012). Disability stage was rated based on the spinocerebellar degeneration functional score (Anheim et al., 2009). The Spinocerebellar Ataxia Functional Index (SCAFI) comprises timed motor tests including the 8 m walk test (8 mW), the 9-hole peg test (9HPT) to measure manual dexterity, and the rate of repeating the syllables PATA within 10 sec to evaluate speech articulation speed (Schmitz-Hübbsch et al., 2008). Participants were screened for depression and anxiety symptoms using the questionnaires Hospital Anxiety and Depression Scale (HADS; scores 8–10 indicating borderline, and ≥ 11 elevated scores), and the Beck Depression Inventory (BDI-II; scores 14–19 considered mild, 20–28 moderate, and 29–63 severe depressive symptoms).

Neuropsychological testing was performed in a subgroup of German-speaking participants (up to 30 patients and 29 controls; Table 2) and included the Montreal Cognitive Assessment (MoCA) as a screening tool for general cognitive impairment (Nasreddine et al., 2005), the short version of the California Verbal Learning Test (CVLT) (Niemann et al., 2008), the digit-span test (forward and backward), and the Paced Auditory Serial Addition Test (PASAT) (Gronwall, 1977) with a 3 sec interval pace. The Color-Word-Interference Test (Stroop) includes a word-reading, color-naming, and interference condition (Bäumler, 1985). To account for speech slowness, we calculated a nomination and interference index using a regression-based correction for reading and naming speed, respectively (Bäumler, 1985). Verbal fluency tests encompassed both phonemic (letter *M*, letter switching *H-T*) and semantic conditions (category *animals*, category switching *sports-fruits*), in each of which participants were asked to generate as many words as possible within two minutes (Strauss et al., 2006).

2.3. MR imaging data acquisition

MRI data collection was carried out utilizing a 3T whole-body scanner (Siemens Healthineers, Erlangen, Germany). Four patients with FRDA were scanned using a Trio scanner, and due to an upgrade, the remaining participants were scanned using a Prisma model. High-resolution T1-weighted anatomical scans were acquired using a magnetization-prepared rapid gradient echo sequence with the

following parameters: TR=2400 ms, TE=2.36 ms, TI=1000 ms, flip angle=8°, voxel resolution=0.8 mm isotropic, number of slices=208, slice thickness=0.8 mm, slice gap=0 mm, FOV=224×224×166.4mm³ on the Prisma scanner, and TR=2300 ms, TE=2.98 ms, TI=900 ms, flip angle=9°, voxel resolution = 1.0 mm isotropic, number of slices=176, slice thickness=1.0 mm, slice gap=0 mm, FOV=256×240×176mm³ on the Trio scanner. Functional imaging at rest was conducted using a gradient echo-planar imaging sequence with TR=2.21 s, TE=30 ms, flip angle=90°, voxel size=3.1 × 3.1 × 3.1 mm, number of slices=36, slice thickness=3.1 mm, slice gap=0.465 mm, FOV=200×200×128.34mm³, and 205 volumes on the Prisma, and TR=2.2 s, TE=30 ms, flip angle=90°, voxel size=3.1 × 3.1 × 3.1 mm, number of slices=36, slice thickness=3.1 mm, slice gap=0.465 mm, FOV=200×200×128.34mm³, and 270 volumes on the Trio. During the functional scan, ambient light was reduced, and participants were instructed to keep their eyes open and avoid focusing on specific thoughts, with the goal of capturing intrinsic brain activity without directed tasks or stimuli.

2.4. Processing of imaging data

T1-weighted anatomical scans and rs-fMRI scans underwent quality check (QC) using MRIQC (v.23.1.0) (Esteban et al., 2017) and were visually examined for potential artifacts. For functional data, exclusion criteria were uniformly applied if motion framewise displacement (mFD) exceeded 0.30 mm. Additionally, a two-tiered QC strategy was employed to ensure effective quality assessment. First, a permissive approach was used to identify significant motion outliers, defined as those with mFD greater than 0.55 mm, with exclusions applied as necessary (Parkes et al., 2018). Subsequently, a stricter criterion was enforced, leading to participant exclusion if any of the following conditions were met: (i) mFD exceeding 0.30 mm, (ii) >20% of the frames had an FD greater than 0.2 mm, or (iii) any FD exceeded 5 mm (Parkes et al., 2018). Participants who satisfied these QC criteria were retained for further processing. All available subjects were included for the structural analysis, whereas the functional analysis included 40 controls and 32 individuals with FRDA.

2.5. Functional MRI data

The rs-fMRI data were preprocessed using the fMRIPrep pipeline (v23.1.3) following our previously published protocol (Dadsena et al., 2025). After preprocessing the functional data with fMRIPrep, we used the CONN toolbox (version conn22v2407) in MATLAB to perform denoising and smoothing, with additional processing implemented via custom scripts written to automate and manage the analysis workflow (Nieto-Castanon and Whitfield-Gabrieli, 2022). We used confounds identified during fMRIPrep preprocessing to remove unwanted signals from the data. For denoising, we applied a standard process that removed potential sources of noise, including signals from white matter (5 components), cerebrospinal fluid (5 components), session effects and their first-order derivatives (2 components), and general trends (3 components). After that, we filtered the BOLD timeseries to keep frequencies between 0.008 Hz and 0.09 Hz to focus on meaningful brain activity. Finally, we applied spatial smoothing to the functional data using a Gaussian kernel with an 8 mm full width at half maximum (Nieto-Castanon, 2020; Nieto-Castanon and Whitfield-Gabrieli, 2022). Using these preprocessed data, we conducted ALFF and fALFF analyses to identify regions with increased or decreased neural activity. ALFF analysis measured the amplitude of low-frequency fluctuations in the BOLD signal, calculated as the root mean square (RMS) of the preprocessed BOLD signal (after the single denoising and band-pass filtering steps described above), with values standardized across participants (Yang et al., 2007). Similarly, the fALFF analysis calculated the ratio of low-frequency signal variability after filtering to the variability before filtering, providing a fractional measure of activity that was also standardized for each participant (Zou et al., 2008). These approaches

enabled us to pinpoint specific regions showing altered neural activity, which were used for ROI-to-ROI analysis to examine functional connectivity differences between patients and controls (Nieto-Castanon and Whitfield-Gabrieli, 2022). Connectivity was estimated between pairs of regions from the Harvard-Oxford atlas. The strength of connectivity between BOLD signals in each pair of regions was expressed using Fisher-transformed correlation coefficients, derived from a general linear model. To compensate for transient effects at the beginning of each scan, the data were weighted using a hemodynamic response model. This combined approach enabled a comprehensive assessment of functional brain alterations by capturing regional activity through ALFF and fALFF, and large-scale network dynamics via ROI-to-ROI connectivity analysis. By integrating these complementary measures, we were able to uncover both localized and distributed functional disruptions, offering deeper insights into the neural mechanisms underlying FRDA.

2.6. Structural MRI data

For structural MRI data, whole-brain segmentation was performed using FastSurfer (v.2.3.0), a deep learning-based neuroimaging pipeline to extract structural metrics from MRI data (Henschel et al., 2020). This process generated volumetric and cortical thickness measurements for 95 anatomically defined regions, including cortical, subcortical and cerebellar structures. Following segmentation, volumetric measurements of subcortical structures were extracted from the automatic segmentation atlas, cortical thickness and volumetric metrics from the automatic segmentation and Desikan-Killiany-Tourville atlas, and cerebellar segmentation from the CerebNet atlas (Henschel et al., 2022). To account for individual variability in brain size, all extracted measures were adjusted for total intracranial volume.

2.7. Statistical analysis

Structural and functional data were statistically analyzed using a General Linear Model (GLM). Age, sex, and scanner model were included as covariates in all analyses. Additionally, we performed a separate analysis after excluding the four patients who were scanned on the Trio scanner. Statistical significance was assessed at a threshold of $p \leq 0.05$, and multiple comparison errors were controlled using the Benjamini-Hochberg (false discovery rate, FDR) correction. Structural group differences were analyzed in R (v.4.3.1) using GLM with age, sex, and scanner as covariates. For functional data, group-level analyses were performed using the CONN toolbox in MATLAB (v.R2022a) (Nieto-Castanon and Whitfield-Gabrieli, 2022). ALFF, fALFF, and ROI-to-ROI connectivity were modeled with second-level random-effects GLM using the same covariates. For each individual connection, a separate GLM was estimated with first-level connectivity measures as dependent variables. Connection-level hypotheses were tested using multivariate parametric statistics with random-effects across subjects, incorporating sample covariance estimation across multiple measurements. Clusters (groups of similar connections) were defined via complete-linkage hierarchical clustering that combined anatomical proximity and functional similarity, and cluster-level inferences were performed within and between functional networks using CONN's cluster-wise procedures. Finally, we applied Spearman's correlation coefficients to examine the relationships between structural, functional, clinical and neuropsychological measures. Given the rarity of FRDA and its multi-domain clinical phenotype, a broad brain-behavior correlation approach was adopted to investigate potential associations between functional network alterations and behavioral measures in an exploratory approach (Bender and Lange, 2001; Glickman et al., 2014). All regions showing structural or functional between-group differences at an uncorrected $p \leq 0.05$ were included in subsequent correlation analyses; the resulting correlations were then FDR-corrected across all examined regions (not across clinical or cognitive scores).

3. Results

3.1. Clinical and neuropsychological assessments

Demographic and clinical characteristics of study participants are reported in Table 1. There were no significant differences with respect to age, sex or handedness when comparing 37 individuals with FRDA and 41 controls. 25 patients were ambulatory with or without support (e.g., walker or crutches) and 12 were unable to walk. Compared to controls, patients showed higher depression scores in both the HADS and BDI-II, while anxiety scores in patients did not differ significantly from controls. Two patients had elevated depression and anxiety scores (one patient with severe, one with moderate depressive symptoms), and seven patients scored in the borderline range. HADS scores correlated significantly with functional impairment in ADL ($r_s=0.377$, $p = 0.023$).

A subgroup of participants (Table 2) underwent cognitive testing with no significant differences in age, sex, handedness or education between patients and controls. Patients performed significantly worse than controls in the MoCA screening, with two patients scoring below cutoff (21 and 25, respectively). No differences between groups were observed in verbal learning, whereas scores in digit-span, PASAT, and all phonemic and semantic verbal fluency tasks were significantly reduced in patients compared to controls. Importantly, slower performances in all Stroop subtests correlated with PATA-repeats, SARA-speech, and SARA-total (Supplementary Table S1). Speed-corrected nomination and selectivity indices of the Stroop test on the other hand did not show significant between-group differences. Remaining cognitive scores were not associated with speech or other clinical measures (Supplementary Table S1).

3.2. Structural brain differences

Significant volume reductions in individuals with FRDA compared to controls were found particularly in the brainstem (including medulla oblongata, pons and mesencephalon), the bilateral cerebellar white matter, left cerebellar lobule V and X, and in the left thalamus (Fig. 1, Supplementary Table S2). Accordingly, cerebrospinal fluid related spaces, including the third and fourth ventricles, were significantly

enlarged in patients compared to controls. Findings remained consistent after excluding the three participants scanned using the Trio scanner. Note that additional regions showed reduced volumes in patients compared to controls, in cerebellar gray matter (right lobule VI, Crus II, X), right thalamus and ventral diencephalon, and cerebral cortex (bilateral precentral gyrus, right middle frontal, left occipital and anterior cingulate cortex), which however did not remain significant after correction for multiple comparisons (Supplementary Table S2).

3.3. Functional brain differences

ALFF analysis revealed increased spontaneous neural activity in individuals with FRDA relative to controls in the bilateral dorsal striatum, centered in the putamen and extending to the caudate, and in medial frontal regions, including the paracingulate and the juxtapositional lobule cortex (i.e., supplementary motor area, SMA). In contrast, decreased ALFF was identified in the left temporal pole and right lateral occipital cortex (Fig. 2A, Supplementary Table S3). fALFF analysis showed increased activity in patients compared to controls in left cerebellar lobules Crus I, Crus II, and lobule VI, as well as in the frontal pole bilaterally (Fig. 2B, Supplementary Table S4). Decreased activity was detected in the left temporal pole and temporal fusiform cortex extending to the hippocampus, as well as in the right superior frontal gyrus and lateral occipital cortex. These regions of altered local neural activity, and additionally regions showing volume reductions in patients compared to controls (i.e., cerebellar lobules V, VI, thalamus, precentral gyrus), were subsequently subjected to ROI-based functional connectivity analyses.

Functional connectivity analysis revealed a pattern of decreased cerebro-cerebellar connectivity in patients compared to controls, whereas connectivity within the cerebellum and between cerebral regions was increased (Fig. 2C-D, Supplementary Table S5). In particular, fronto-cerebellar functional coupling between right superior frontal gyrus and the left cerebellar lobule VI, right frontal pole and the left Crus I, as well as the left SMA and the right lobule VI was reduced in patients compared to controls. The only exception to the observed decreased cerebro-cerebellar coupling was that the connectivity between the left hippocampus and ipsilateral cerebellum (Crus I, Crus II) was increased

Table 1
Demographics and clinical characteristics of FRDA patients and controls.

	FRDA patients (n = 37)		Controls (n = 41)		U test	effect size	p
	n	mean (SD)	n	mean (SD)			
Demographics							
Age (years)	37	36.1 (12.1)	41	34.9 (12.8)	714	0.05	0.660
Sex (female/male)	37	20/17	41	24/17	^a 0.159	^a 0.05	^a 0.820
Handedness (right/left) ^b	37	32/5	41	38/3		^a 0.10	^a 0.466
Clinical measures							
Age of onset (years)	37	16.8 (7.2)		n.a.			
Disease duration (years)	37	19.3 (8.9)		n.a.			
Disability stage (0–7)	37	4.7 (1.3)		n.a.			
GAA repeats:							
allele 1:	37	491.7 (210.7)		n.a.			
allele 2:	37	815.2 (199.6)		n.a.			
SARA:	37	19.6 (8.8)		n.a.			
ADL:	37	12.9 (6.2)		n.a.			
INAS:	37	5.4 (2.4)		n.a.			
SCAFI:	20	18.4 (22.0)	21	3.9 (0.7)	13.5	0.80	<0.001
9 hole peg, dominant (sec):	35	61.1 (32.6)	21	17.6 (2.6)	4	0.82	<0.001
non-dominant (sec):	35	71.2 (39.6)	21	18.2 (2.3)	0	0.83	<0.001
PATA (words in 10 sec):	37	22.1 (4.5)	21	35.8 (5.7)	20	0.78	<0.001
HADS:	36	8.5 (6.7)	25	4.4 (4.6)	255	0.37	0.004
anxiety score (0–21):	36	4.8 (4.1)	25	3.2 (2.7)	338.5	0.21	0.101
depression score (0–21):	36	3.7 (3.0)	25	1.2 (2.0)	169.5	0.53	<0.001
BDI-II:	29	7.6 (7.5)	30	2.1 (3.1)	172	0.53	<0.001

FRDA, Friedreich's ataxia; SARA, Scale for the Assessment and Rating for Ataxia; ADL, Activities of Daily Living; INAS, Inventory of Non-Ataxia Symptoms; SCAFI, Spinocerebellar Ataxia Functional Index; HADS, Hospital Anxiety and Depression Scale; BDI-II, Beck-Depression Inventory; n.a., not applicable. ^a Chi-square/Fisher's exact test with Phi as effect size (remaining group comparisons assessed with Mann Whitney U tests and $r = Z/\sqrt{N}$ as effect size)

^b Based on the Edinburgh Inventory (Oldfield, 1971).

Table 2
Subgroups of participants with neuropsychological test performance.

	FRDA patients (n = 30)		Controls (n = 29)		U test	effect size	p
	n	mean (SD)	n	mean (SD)			
Demographics							
Age (years)	30	36.6 (13.0)	29	35.1 (12.9)	411	0.05	0.721
Sex (female/male)	30	17/13	29	17/12	^a 0.023	^a 0.02	^a 1.000
Handedness (right/left) ^b	30	25/5	29	27/2		^a 0.15	^a 0.424
Education: ISCED level	30	3.6 (1.0)	24	4 (1.1)	280	0.20	0.133
MoCA: cognitive screening	29	27.5 (2.0)	29	28.4 (1.9)	286.5	0.28	0.033
Memory and learning							
CVLT:							
total immediate recall	29	30.6 (3.7)	27	31.4 (3.7)	332	0.13	0.332
delayed free recall	29	16.3 (2.3)	27	16.1 (2.2)	358.5	0.08	0.577
cued recall	29	7.9 (1.4)	27	7.9 (1.4)	379.5	0.03	0.827
Attention and working memory							
Digit-span:							
forward	29	7.1 (1.9)	29	9.1 (1.6)	174	0.51	<0.001
backward	29	6.3 (1.4)	29	8.0 (2.1)	214.5	0.43	<0.001
PASAT: correct responses (%)	24	80.8 (13.9)	19	90.4 (13.8)	121	0.40	0.008
Executive functions							
Stroop:							
word reading	29	40.7 (7.9)	29	27.4 (3.8)	37	0.78	<0.001
color naming	29	59.1 (13.1)	29	41.9 (5.8)	57.5	0.74	<0.001
interference	29	94.5 (18.6)	29	68.0 (14.7)	100.5	0.65	<0.001
nomination index	29	54.7 (9.0)	29	51.1 (8.4)	316	0.21	0.105
interference index	29	56.3 (9.5)	29	53.3 (8.4)	345.5	0.15	0.246
Verbal fluency:							
Phonemic -letter M	20	17.2 (4.9)	27	23.6 (5.5)	-0.53	0.53	<0.001
- switching H-T	21	17.9 (6.1)	27	25.1 (5.9)	103.5	0.54	<0.001
Semantic -animals	21	29 (5.8)	27	41.1 (11.1)	-0.55	0.55	<0.001
- sports-fruits	21	19.7 (4.1)	27	25.7 (6.6)	117	0.50	<0.001

FRDA, Friedreich's ataxia; MoCA, Montreal cognitive assessment; CVLT, California verbal learning test – short version; PASAT, Paced Auditory Serial Addition Test.

^a Chi-square/Fisher's exact test with Phi as effect size (remaining group comparisons assessed with Mann Whitney U tests and $r = Z/\sqrt{N}$ as effect size).

^b Based on the Edinburgh Inventory (Oldfield, 1971).

in patients compared to controls. Higher intracerebellar connectivity was mainly observed between lobules VI and Crus II. Patients also exhibited increased coupling between the left thalamus and putamen.

A full list of functional connectivity differences between patients and controls significant at an uncorrected level ($p \leq 0.05$) can be found in Supplementary Table S5, additionally showing decreased striato-cerebellar connectivity (Crus I, Crus II), and increased fronto-thalamic and corticocortical coupling. Results were unchanged when participants scanned on the Trio system were excluded.

3.4. Correlations of structural and functional brain changes with clinical measures

Exploratory brain-behavior correlations showed that regional volume reductions were significantly associated with disease severity (Fig. 3): In particular, strong correlations ($|r_s| \geq 0.50$) were observed between lower cerebellar white matter volumes and higher scores on disability stage, SARA, and INAS; lower gray matter volumes of cerebellar lobule X were associated with longer disease duration and worsening in clinical ratings, and lower thalamic volumes with longer disease duration. Poorer performances in SCAFI subtests (9hpt, PATA) were mostly related to cerebellar and thalamic volume loss. For cognitive measures, we found strong correlations of Stroop subtests with cerebellar white matter and anterior cingulate cortex, and lower performances in MoCA showed moderate associations with volume loss in the brainstem, cerebellum and thalamus. Stroop indices corrected for speech slowness and other cognitive scores showed no relationship with structural measures.

Correlations with functional connectivity measures showed mostly moderate associations with clinical and cognitive scores ($|r_s| \geq 0.36$) and indicated the following pattern: Higher disease severity was related to decreased cerebro-cerebellar coupling and increased intracerebellar/intracerebral coupling, respectively (Fig. 4). For instance, SMA-cerebellar and putaminal-cerebellar connectivity was lower in patients with higher disability, SARA scores, and worse performance in SCAFI subtests (9hpt, PATA), whereas thalamo-striatal connectivity increased

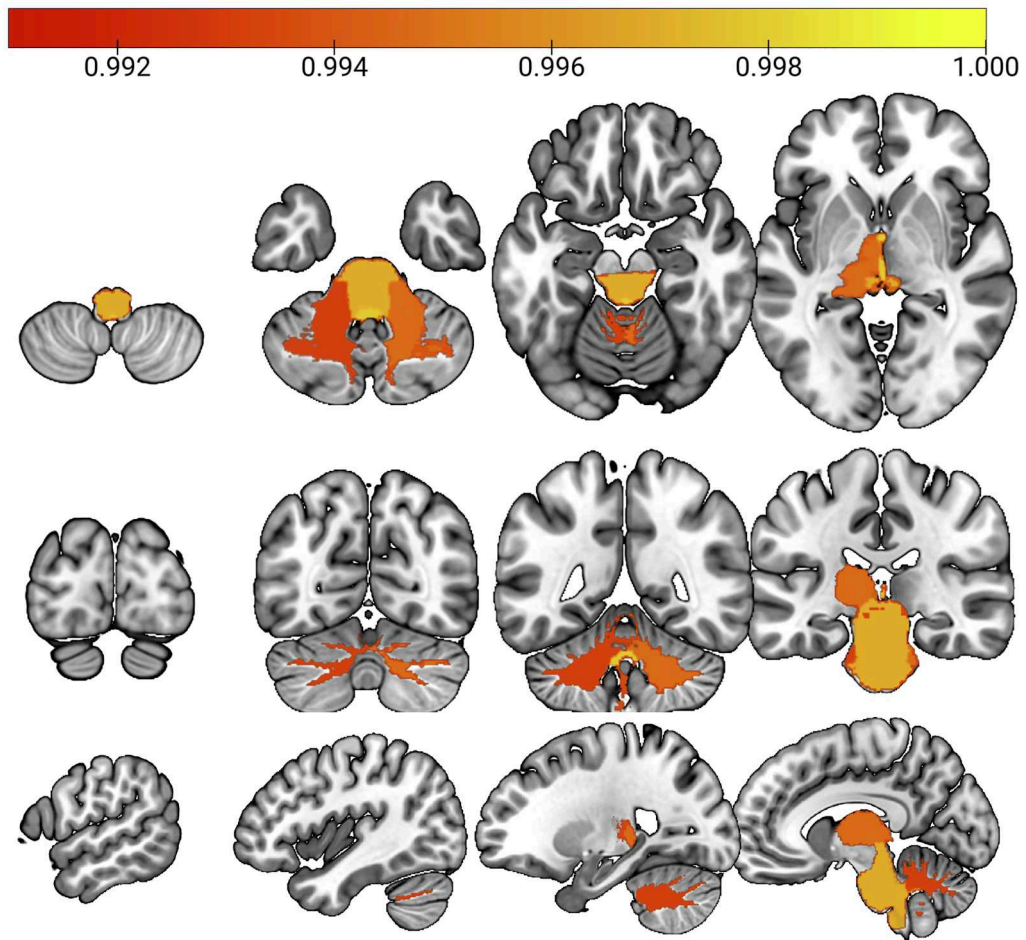
with higher scores of disabilities, ADL, INAS and 9hpt. Decreased connectivity between the precentral gyrus and contralateral cerebellum VI as well as increased intracerebellar coupling (VI, Crus I) were associated with longer disease duration. Similarly, for cognitive measures we found that lower performances in Stroop and phonemic verbal fluency were linked to reduced fronto-cerebellar connectivity in patients. Notably, lower performances in both Stroop and SCAFI subtests were associated with decrease in connectivity between the precentral gyrus and cerebellum (VI, Crus I). Lower scores in digit-span were linked to increased intracerebellar coupling (Crus I/II with VI), while increased connectivity between the hippocampus and cerebellar Crus I/II was related to better digit-span and Stroop interference. Higher hippocampal-cerebellar along with decreased fronto-cerebellar coupling was also related to elevated scores in mood questionnaires (BDI-II, HADS).

Finally, cross-modal correlation between functional connectivity and structural data indicated that lower cerebellar gray matter volumes correlated with lower fronto-cerebellar connectivity, whereas the more pronounced volume reductions in the brainstem, cerebellar white matter and thalamus were associated with increased intracerebellar and intracerebral coupling (Fig. 4). Volumes of cerebellar lobule V on the other hand showed a positive association with increased connectivity within the cerebellum.

4. Discussion

This study presents a multimodal resting-state and structural MRI analysis in individuals with FRDA, aiming to better understand the interplay between brain structure, spontaneous activity, and functional connectivity in relation to clinical symptoms. Overall, patients with FRDA showed decreased fronto-cerebellar connectivity together with increased intra-cerebellar, hippocampal-cerebellar and thalamo-striatal coupling. While structural volume loss showed stronger associations with clinical disease severity, alterations in functional coactivation could better explain performances on cognitive tests. Increases in functional connectivity were related to more severe clinical symptoms and greater infratentorial degeneration but were in part also associated

(A)



(B)

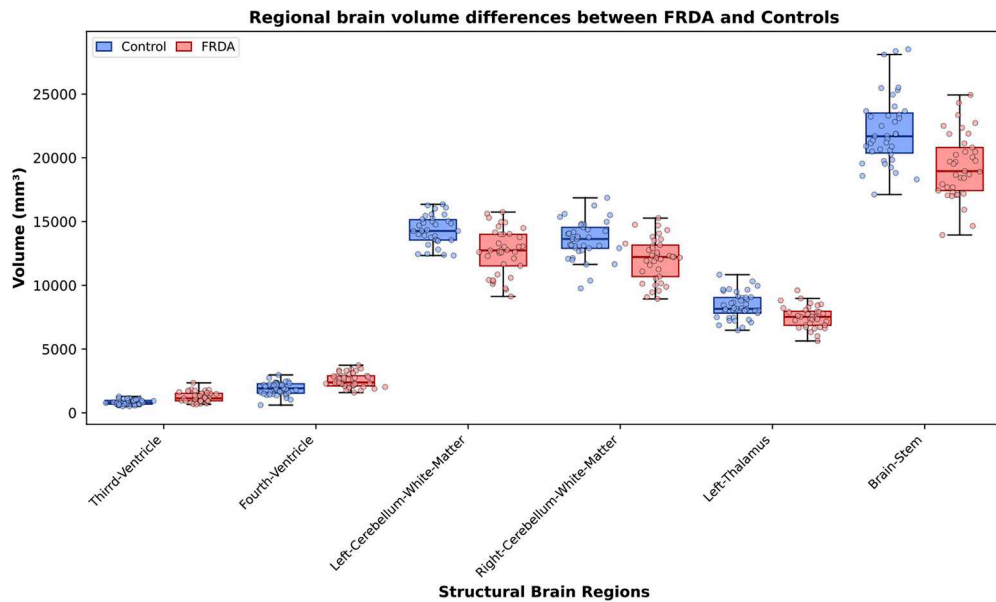


Fig. 1. Structural brain differences between patients with Friedreich’s ataxia (FRDA) and controls. (a) Highlighted brain regions with significant volumetric differences ($p \leq 0.05$, FDR corrected) displayed across coronal, sagittal, axial views. The color scale reflects p-values, with warmer colors indicating higher significance. The box plot illustrates the volumes for the significant brain regions, showing the distribution across subjects in each group.

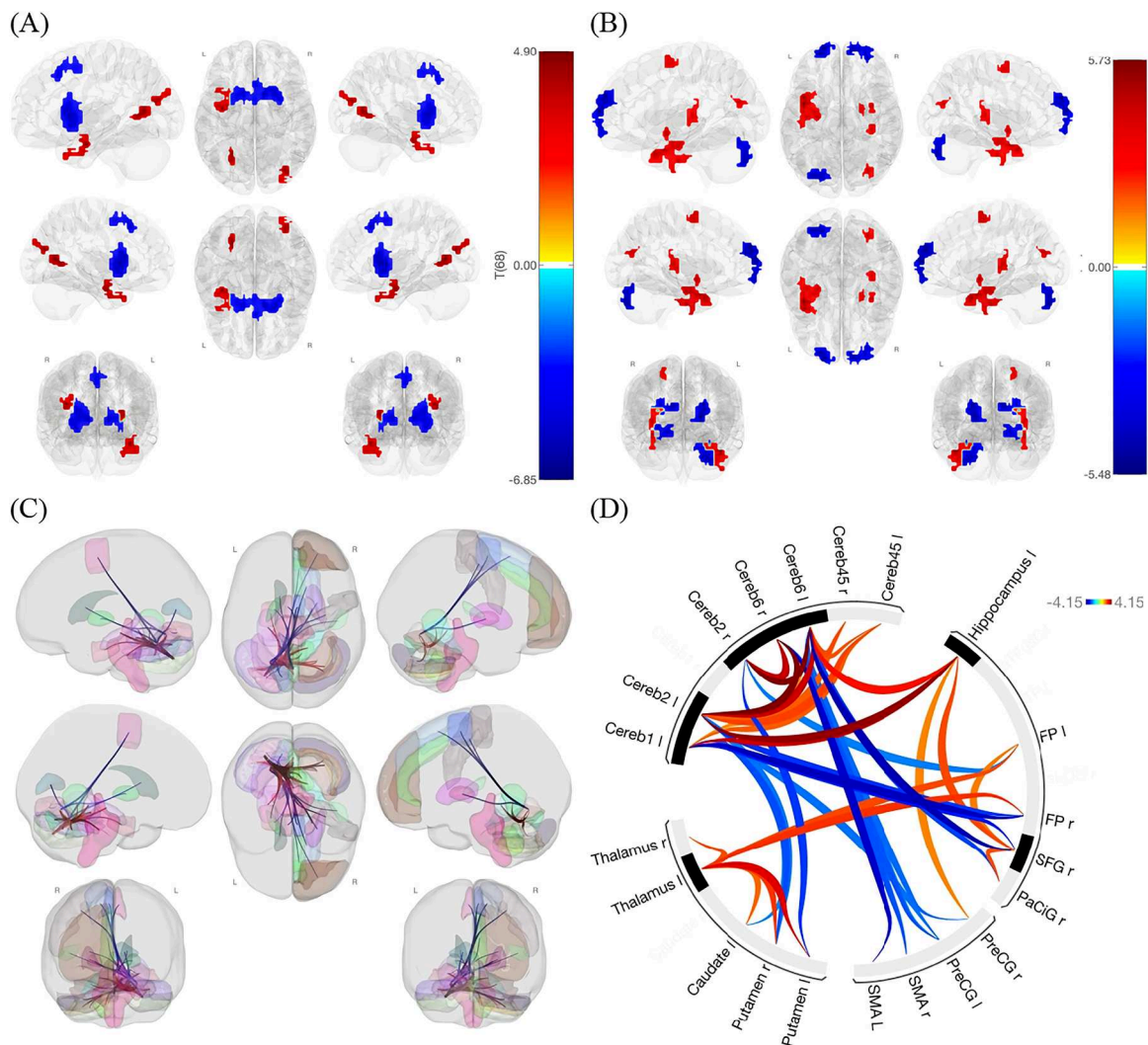


Fig. 2. Functional activity and connectivity differences between patients with Friedreich's ataxia (FRDA) and controls (a) amplitude of low-frequency fluctuations (ALFF) results showing frequency-specific alterations in spontaneous neural activity; red denotes increased and blue denotes decreased activity (cluster-level corrected at $p \leq 0.05$). (b) fractional ALFF (fALFF) results highlighting additional frequency-dependent changes in neural activity (cluster-level corrected at $p \leq 0.05$). (c) ROI-to-ROI functional connectivity maps illustrating increased (red) and decreased (blue) connections between brain regions. (d) Circular visualization of altered functional connections, with red indicating increased and blue indicating decreased connectivity ($p \leq 0.05$, FDR-corrected).

with improved cognitive performances. This dissociation may reflect compensatory functional enhancement that could help sustain function in the presence of progressive structural damage and clinical impairment. Taken together, our findings indicate widespread disruptions in both long-range and intraregional network connectivity with potential adaptive reorganization patterns, offering complementary insights into the systems-level consequences of cerebellar and brainstem degeneration.

The results of this study align with existing literature on structural brain changes and the cognitive profile in FRDA, and importantly, extend previous rs-fMRI studies on functional connectivity alterations. Consistent with morphometric findings in FRDA (Adanyeguh et al., 2023; Georgiou-Karistianis et al., 2025; Harding et al., 2021), regional volume reductions were observed in the brainstem (including medulla, pons, mesencephalon), bilateral cerebellar white matter surrounding the cerebellar deep nuclei, left hemispheric lobules V and X, and left thalamus, along with ventricular enlargement. Infratentorial and thalamic volume loss was strongly related to greater clinical disease severity and worse motor performance. Regarding cognitive measures, poorer Stroop-interference performance in particular was associated with lower volumes in cerebellar white and the anterior cingulate cortex, which

plays a critical role in conflict monitoring and error detection during the Stroop-test (Botvinick et al., 2004). Hence, subtle volume reductions observed in the anterior cingulate may contribute to executive disabilities, rather than dysarthria-related impairment due to infratentorial degeneration alone.

Functionally, we observed both decreased and increased connectivity alterations in patients compared to controls. The few published rs-fMRI studies in FRDA employed clinically comparable groups of participants and demonstrated reduced cerebro-cerebellar connectivity, generally in line with our findings (Cocozza et al., 2018; Kerestes et al., 2023). Cocozza et al. (2018) reported decreased fronto-cerebellar coupling of the medial frontal gyrus with cerebellar lobule VI and vermis, whereas connectivity between cortical regions was increased (Cocozza et al., 2018). Kerestes et al. (2023) found reduced connectivity of the anterior cerebellum (lobules I-V) to pre- and postcentral gyri that was associated with disease severity and motor impairment; as well as reduced connectivity between the superior posterior cerebellum (lobules VI-VII) and the left dorsolateral prefrontal cortex (Kerestes et al., 2023). Similarly, we observed reduced connectivity of the right superior frontal gyrus, bilateral frontal pole and SMA predominantly with the contralateral posterior cerebellar lobules VI, Crus I and II. Decreased

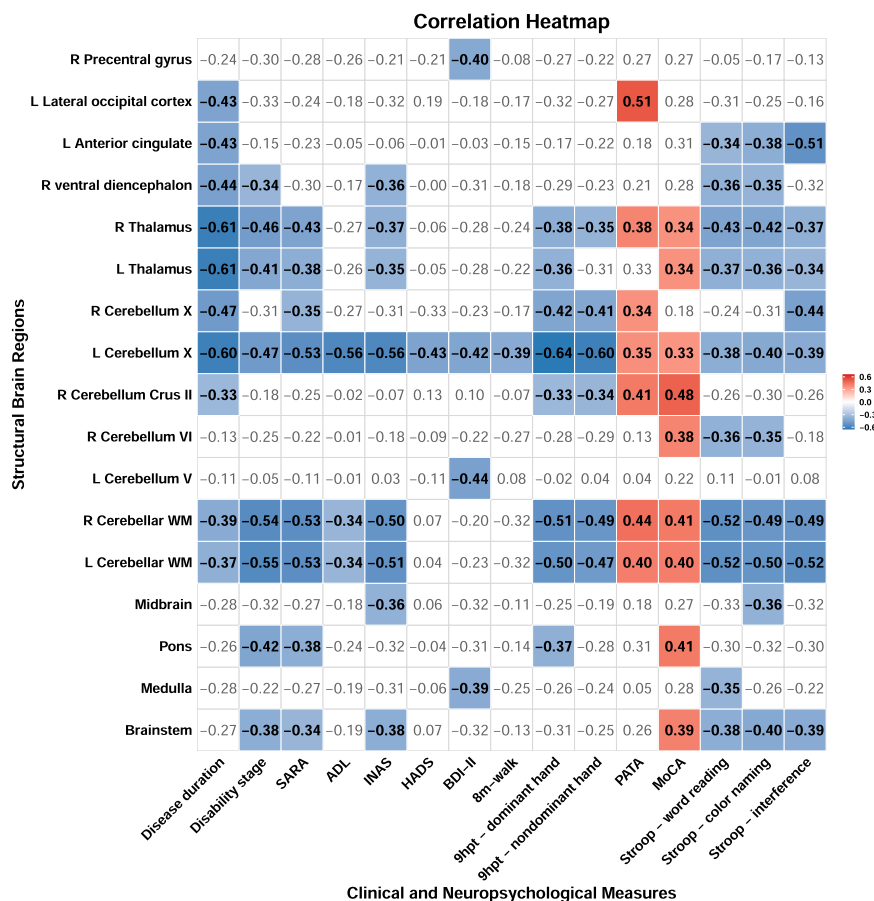


Fig. 3. Correlation heatmap between volumes of structurally altered brain regions with clinical and cognitive measures in patients with Friedreich’s ataxia; significant correlation at $p \leq 0.05$ (FDR-corrected across regions) in bold and color-coded. Listed anatomical regions include regions with group differences at $p \leq 0.05$, either FDR-corrected or uncorrected (see Supplementary Table S2). Note that higher scores in disability, SARA, ADL, INAS, HADS, BDI-II, 8m-walk, 9hpt, Stroop indicate greater impairment, whereas lower scores in PATA, MoCA indicate greater impairment.

Abbreviations: R = right; L = left; WM = white matter; SARA = Scale for the Assessment and Rating of Ataxia; ADL = Activities of Daily Living; INAS = Inventory of Non-Ataxia Signs; HADS = Hospital Anxiety and Depression Scale; BDI-II = Beck Depression Inventory II; PATA = PATA repetition rate; 8m-walk = 8-meter walking test; 9HPT = 9-Hole Peg Test; MoCA = Montreal Cognitive Assessment.

connectivity with the primary motor cortex in the precentral gyrus, and increased cortico-cortical coactivation were evident only at the uncorrected level. Lower cerebellar gray matter and greater disease severity were moderately associated with decreases in fronto-cerebellar connectivity. While volumetric correlations with impaired functional coupling cannot directly confirm tract-specific damage, Kerestes et al. (2023) could show that weaker anterior cerebellar connectivity with the motor cortex was related to reduced integrity in cerebello-cerebral pathways including the superior cerebellar peduncles (Kerestes et al., 2023). We additionally found moderate associations of reduced fronto-cerebellar connectivity with impaired cognitive performance, including phonemic fluency and Stroop tasks, reinforcing the well-recognized role of cerebro-cerebellar communication in executive functioning (Bellebaum and Daum, 2007; Schmahmann and Sherman, 1998). Our findings therefore not only confirm functional disturbances in motor and executive cortico-cerebellar systems but also provide first evidence that dysfunctional coactivation at rest between the posterior cerebellum and the prefrontal cortex is linked to impaired cognitive control in FRDA.

In addition to decreased fronto-cerebellar connectivity, we found increased coactivation between the left hippocampus and ipsilateral cerebellar lobules Crus I and II. This enhanced coupling was in particular associated with better attentional performance. Importantly, fALFF analysis revealed reduced local activity in the left hippocampus in patients relative to controls, whereas activity in cerebellar Crus I and II was

increased. It is therefore possible that the diminished hippocampal synchronization may elicit a compensatory response characterized by enhanced cerebellar activity and hippocampal-cerebellar coupling, potentially supporting cognitive processing. Within the cerebellum, lobules Crus I/II are specifically involved in cognitive functioning, and the hippocampus contributes to memory-dependent aspects of cognitive control (Bègue et al., 2024; Rubin et al., 2014; Schmahmann and Sherman, 1998). However, given the exploratory nature of correlations, future studies are needed to test the hypothesis of an enhanced and possibly compensatory role of hippocampal-cerebellar connectivity in FRDA. Notably, the ipsilateral (left-left) hippocampal-cerebellar coupling deviates from the typical contra-lateral organization of cerebro-cerebellar circuits crossing via pontine relays. Anatomical and recent large-scale rs-fMRI studies, however, show that both the left and right hippocampi maintain bilateral connections to widespread cerebellar regions, although contralateral functional coupling tends to be stronger (Apasamy et al., 2025).

The increase in cerebellar activity and intra-cerebellar hyperconnectivity, particularly between cerebellar lobules VI and Crus II, is consistent with our previous task-based findings during speech and executive processing (Dogan et al., 2016). Conversely, Tranfa et al. (2025) reported diminished network integration in vermal lobule VIII using graph-theoretical measures (Tranfa et al., 2025), which might point to differential recruitment patterns of lateral versus midline/vermal cerebellar nodes. Higher intracerebellar co-activation showed a mixed

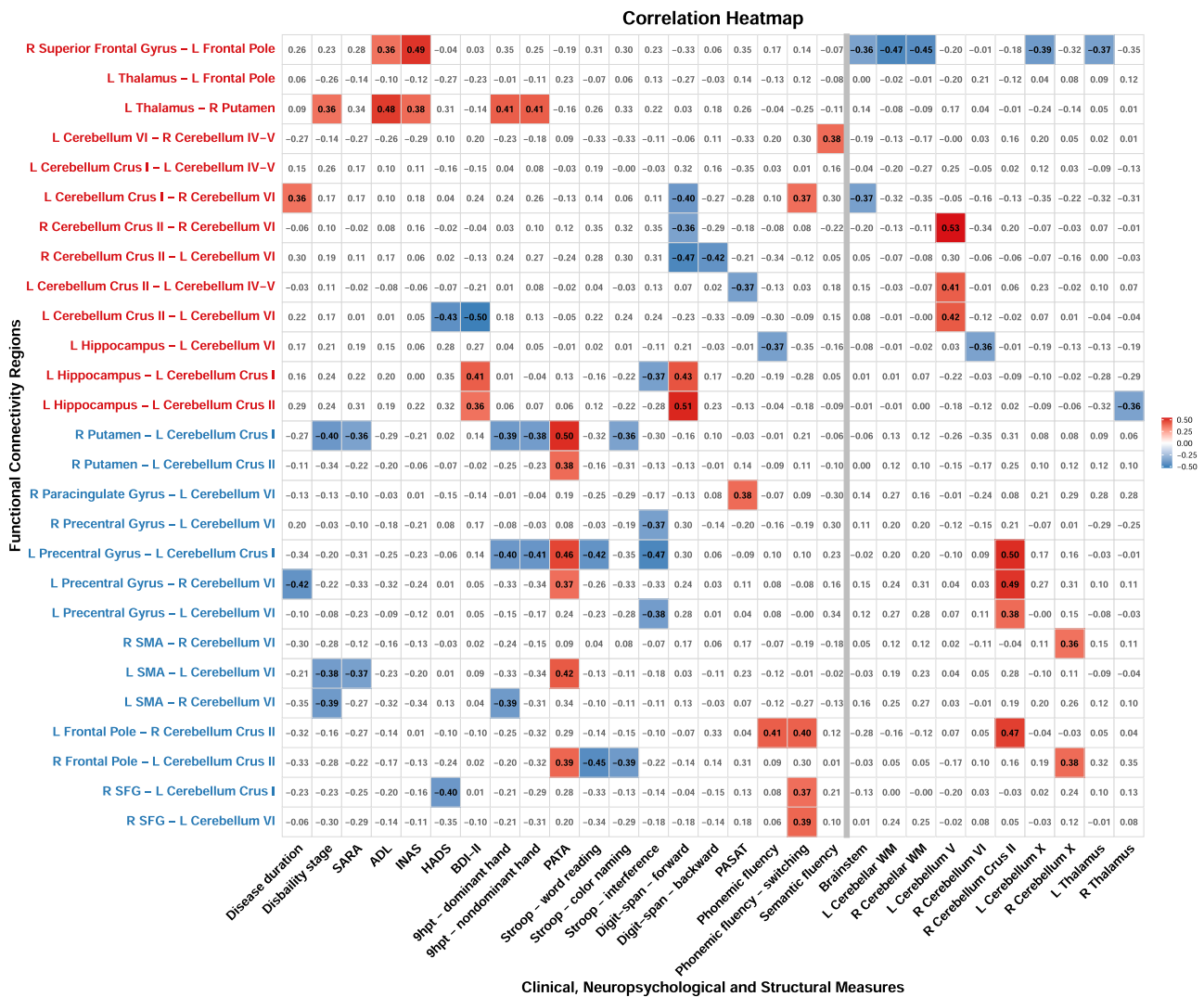


Fig. 4. Correlation heatmap between ROI-to-ROI functional connectivity metrics and clinical, cognitive measures and volumes of structurally altered brain regions in patients with Friedreich’s ataxia; significant correlation at $p \leq 0.05$ (FDR-corrected across regions) in bold and color-coded. Listed ROI-to-ROI connections include connectivity results with group differences at $p \leq 0.05$, either FDR-corrected or uncorrected (see Supplementary Table S5). ROI-to-ROI connections in blue: lower connectivity in patients compared to controls; in red: higher connectivity in patients compared to controls. Note that higher scores in disability, SARA, ADL, INAS, HADS, BDI-II, 9hpt, Stroop indicate greater impairment, whereas lower scores in PATA, digit span, PASAT, verbal fluency indicate greater impairment. Abbreviations: ADL = Activities of Daily Living; BDI-II = Beck Depression Inventory II; HADS = Hospital Anxiety and Depression Scale; INAS = Inventory of Non-Ataxia Signs; SARA = Scale for the Assessment and Rating of Ataxia; PATA = PATA repetition rate; PASAT = Paced Auditory Serial Addition Test; L = Left; R = Right; SMA = Supplementary Motor Area; SFG = Superior Frontal Gyrus.

pattern of associations with executive functions (i.e., linked to better performance in verbal fluency, but worse working memory). Thus, it remains unclear whether cerebellar hyperconnectivity reflects functional reorganization to support function, possibly with domain-specific limits where enhanced intra-cerebellar recruitment may no longer be beneficial or even maladaptive (e.g., more demanding working memory tasks).

Patients further exhibited increased thalamo-striatal co-activation, while the striatum showed a tendency toward reduced connectivity with Crus I/II. Previous fMRI studies have reported stronger striatal activity during motor task performance in FRDA compared to controls (Ginestroni et al., 2012; Harding et al., 2017), and likewise our ALFF analyses showed increased spontaneous activity in the striatum at rest. Greater thalamo-striatal coupling was related to clinical impairment, indicating that connectivity increases emerge in the context of advanced disease severity. The cerebellum and basal ganglia form an integrated, bidirectionally connected network via thalamic and pontine relays, allowing functional compensation when one system is compromised

(Bostan et al., 2010; Bostan and Strick, 2018). We recently also demonstrated alterations in microstructure and energy-metabolism along the dentato-thalamo-cortical pathway in FRDA, with increased effective functional dentato-thalamo connectivity to possibly maximize cerebellar activity (Jing et al., 2025). From this perspective, thalamo-striatal strengthening in individuals with higher disability may represent adaptive recruitment of basal ganglia loops in response to dentato-thalamo-cortical pathway degeneration.

Taken together, our findings support the hypothesis of disruptions in motor and executive cortico-cerebellar circuits, possibly due to primary infratentorial pathology, and suggest the presence of functional regulation in FRDA when cerebro-cerebellar pathways are compromised. Importantly, compensatory enhancement should not be inferred solely from associations with disease pathology, but should ideally be supported by evidence that it contributes to functional maintenance or improved behavioral performance (Cabeza et al., 2018). Exploratory brain-behavior associations indicated both, i.e. increased functional co-activation was linked to infratentorial degeneration, and to a certain

extent to better executive functioning. This, at least in part, supports the notion that increased coupling may reflect compensatory/adaptive reorganization, rather than purely pathology-driven neural dedifferentiation (Dogan et al., 2016; Vavla et al., 2022). Notably, whereas brain volume loss showed strong associations with clinical disease severity, the widespread functional network alterations could not be adequately explained by volumetric changes alone and appeared to be critical for understanding how cognitive changes are affected by both large-scale and intra-regional network organization.

A relevant strength of our work is that we used regional spontaneous activity indices along with areas of structural decline to define seed regions for connectivity analyses, thereby adding insight into network-level findings and supporting the interpretation of potential reorganization patterns (e.g., striatal, hippocampal connectivity). Previous rs-fMRI studies have focused on several cortical or cerebellar ROI for seed-to-voxel analyses (Cocozza et al., 2018; Kerestes et al., 2023). ALFF and fALFF measures are well-established, physiologically meaningful markers of local low-frequency BOLD oscillations, and have been shown in other neurodegenerative conditions, such as Alzheimer's disease, to capture clinically relevant regional alterations, often co-varying with disrupted connectivity and cognitive decline (Han et al., 2011; Jia et al., 2020; Yang et al., 2018). In our study, ALFF and fALFF effects revealed additional areas of both increased and decreased intrinsic neural activity without concomitant regional structural abnormalities, reinforcing that local neural activity is essential to inform about network hubs and breakdown of long-range communication. Hence, the integrative analysis of regional spontaneous activity and functional connectivity, together with regional structural decline, provides a comprehensive approach contributing to our understanding of how functional alterations emerge, interact and where degenerative versus compensatory dynamics may predominate.

Nevertheless, several limitations remain. Missing data, particularly for performance-based and cognitive measures, occurred for diverse reasons (including physical limitations, fatigue, time constraints). To ensure transparency and facilitate interpretation of findings, detailed sample sizes are reported for all analyses. The cross-sectional and exploratory design precludes conclusions about causality, temporal dynamics, or a clear distinction between compensatory and maladaptive processes. Although anchoring connectivity analysis to regions with altered activity improves specificity, it may miss broader network-level changes that are better captured by whole-brain approaches. To control for false positives, we applied FDR correction where appropriate; however, for brain-behavior correlations we additionally examined uncorrected effects in an exploratory manner to characterize broader functional association patterns and did not adjust across clinical or cognitive assessments (Bender and Lange, 2001). While this approach yielded valuable insights to inform subsequent hypothesis-driven investigations, future replications using larger cohorts and longitudinal designs, ideally within large-scale multinational initiatives such as ENIGMA-Ataxia (Harding et al., 2021), will be essential to test generalizability, and enable more in-depth, stage-dependent subgroup analyses. This is especially important since most fMRI studies include adult participants, leaving neurodevelopmental aspects of functional brain changes in pediatric FRDA largely unexplored.

In summary, our findings offer a coherent and clinically meaningful account of how FRDA affects brain function at rest. We provide evidence of canonical fronto-cerebellar connectivity disruptions, concomitant with increased thalamo-striatal, intracerebellar and hippocampal-cerebellar coupling that appears to support compensatory processes for certain cognitive functions. These results highlight broader functional network alterations in FRDA that extend beyond focal degeneration and may play a key role in shaping both motor and cognitive outcomes. From a translational perspective, targeted connectivity analyses may offer sensitive tools for disease monitoring and mechanistic readouts in clinical trials, especially for therapies that aim to preserve cerebellar output or rebalance network function. Taken

together, our results support the view that FRDA is best understood as a distributed network disorder, in which degeneration of cerebellar efferents disrupts long-range integration, while additional circuits may be recruited, potentially reflecting adaptive reorganization as disability progresses.

Consent statement

All human subjects provided informed consent prior to participation in this study.

Further FACROSS study group members

Kerstin Konrad (Section Child Neuropsychology, Department of Child and Adolescent Psychiatry, Psychosomatics and Psychotherapy, University Hospital, RWTH Aachen); Miguel Pishnamaz, Maximilian Praster (Department for Orthopaedics, Trauma and Reconstructive Surgery, University Hospital RWTH Aachen); Thomas Clavel (Functional Microbiome Research Group, Institute of Medical Microbiology, University Hospital RWTH Aachen); Vera Jankowski, Joachim Jankowski (Institute for Molecular Cardiovascular Research, University Hospital RWTH Aachen); Oliver Pabst (Institute of Molecular Medicine, University Hospital RWTH Aachen); Katharina Marx-Schütt, Nikolaus Marx, Julia Möllmann, Malte Jacobsen (Department of Internal Medicine I, Cardiology, University Hospital RWTH Aachen); Juergen Dukart, Simon Eickhoff (Institute of Neuroscience and Medicine, Brain and Behaviour (INM-7), Research Centre Jülich).

Funding

The European Friedreich Ataxia Consortium for Translational Studies (EFACTS) was funded by an FP7 Grant from the European Commission (HEALTH-F2-2010-242193), EuroAtaxia, and Voyager Therapeutics. This work was supported by the Interdisciplinary Center for Clinical Research within the Faculty of Medicine at the RWTH Aachen University, Germany (OC2-2), the Brain Imaging Facility of the IZKF, and by the Friedreich's Ataxia Research Alliance (FARA).

Data and code availability statement

De-identified study data and the analysis code used in this study are available from the corresponding author on reasonable request, subject to institutional and data protection regulations.

CRediT authorship contribution statement

Ravi Dadsena: Writing – review & editing, Writing – original draft, Visualization, Validation, Software, Methodology, Investigation, Formal analysis, Data curation, Conceptualization. **Sandro Romanzetti:** Writing – review & editing, Data curation. **Stella Andrea Lischewski:** Writing – review & editing, Data curation. **Yinghua Jing:** Writing – review & editing. **Dagmar Timmann:** Writing – review & editing, Data curation. **Jennifer Faber:** Writing – review & editing, Data curation. **Jörg B. Schulz:** Writing – review & editing, Resources. **Kathrin Reetz:** Writing – review & editing, Supervision, Project administration, Investigation, Funding acquisition, Data curation, Conceptualization. **Imis Dogan:** Writing – review & editing, Visualization, Project administration, Data curation, Conceptualization.

Declaration of competing interest

KR has received honoraria for presentations or advisory boards from Biogen, Eisai, Lilly and Roche. SAL has received speaking and advisory honoraria from Biogen. JBS received grants from Biogen and Eisai and for presentations or advisory boards from Biogen, Reata, Eisai, Lilly, Roche, NovoNordisk. DT has received grants from the EU, DFG and

Bernd Fink foundation unrelated to the present research.

Acknowledgements

We thank Shahram Mirzazade for his valuable contribution in MRI data acquisition. We are grateful to all the participants who took part in this study.

Supplementary materials

Supplementary material associated with this article can be found, in the online version, at [doi:10.1016/j.neuroimage.2026.121872](https://doi.org/10.1016/j.neuroimage.2026.121872).

References

- Adanyeguh, I.M., Joers, J.M., Deelchand, D.K., Hutter, D.H., Eberly, L.E., Guo, B., Iltis, I., Bushara, K.O., Henry, P.G., Lenglet, C., 2023. Brain MRI detects early-stage alterations and disease progression in Friedreich ataxia. *Brain Commun.* 5, fca196. <https://doi.org/10.1093/braincomms/fca196>.
- Anheim, M., Monga, B., Fleury, M., Charles, P., Barbot, C., Salih, M., Delaunoy, J.P., Fritsch, M., Arning, L., Synofzik, M., Schöls, L., Sequeiros, J., Goizet, C., Marelli, C., Le Ber, I., Koht, J., Gazulla, J., De Blecker, J., Mukhtar, M., Drouot, N., Ali-Pacha, L., Benhassine, T., Chbicheb, M., M'Zahem, A., Hamri, A., Chabrol, R., Pouget, J., Murphy, R., Watanabe, M., Coutinho, P., Tazir, M., Durr, A., Brice, A., Tranchant, C., Koenig, M., 2009. Ataxia with oculomotor apraxia type 2: clinical, biological and genotype/phenotype correlation study of a cohort of 90 patients. *Brain* 132, 2688–2698. <https://doi.org/10.1093/brain/awp211>.
- Apasamy, K., Berry, S.C., Read, M.L., Ramnani, N., Hodgetts, C.J., 2025. Mapping hippocampal-cerebellar functional connectivity across the human adult lifespan. *Commun. Biol.* 8, 1619. <https://doi.org/10.1038/s42003-025-08972-2>.
- Bäumler, G., 1985. Farbe-wort-interferenztest (FWIT) nach J. R. Stroop.
- Bégué, I., Elandaloussi, Y., Delavari, F., Cao, H., Moussa-Tooks, A., Roser, M., Coupé, P., Leboyer, M., Kaiser, S., Houenou, J., Brady, R., Laidi, C., 2024. The cerebellum and cognitive function: anatomical evidence from a transdiagnostic sample. *Cerebellum* 23, 1399–1410. <https://doi.org/10.1007/s12311-023-01645-y>.
- Bellebaum, C., Daum, I., 2007. Cerebellar involvement in executive control. *Cerebellum* 6, 184–192. <https://doi.org/10.1008/14734220601169707>.
- Bender, R., Lange, S., 2001. Adjusting for multiple testing—when and how? *J. Clin. Epidemiol.* 54, 343–349. [https://doi.org/10.1016/s0895-4356\(00\)00314-0](https://doi.org/10.1016/s0895-4356(00)00314-0).
- Bostan, A.C., Dum, R.P., Strick, P.L., 2010. The basal ganglia communicate with the cerebellum. *Proc. Natl. Acad. Sci.* 107, 8452–8456. <https://doi.org/10.1073/pnas.1000496107>.
- Bostan, A.C., Strick, P.L., 2018. The basal ganglia and the cerebellum: nodes in an integrated network. *Nat. Rev. Neurosci.* 19, 338–350. <https://doi.org/10.1038/s41583-018-0002-7>.
- Botvinick, M.M., Cohen, J.D., Carter, C.S., 2004. Conflict monitoring and anterior cingulate cortex: an update. *Trends Cogn. Sci.* 8, 539–546. <https://doi.org/10.1016/j.tics.2004.10.003>.
- Cabeza, R., Albert, M., Belleville, S., Craik, F.I.M., Duarte, A., Grady, C.L., Lindenberger, U., Nyberg, L., Park, D.C., Reuter-Lorenz, P.A., Rugg, M.D., Steffener, J., Rajah, M.N., 2018. Maintenance, reserve and compensation: the cognitive neuroscience of healthy ageing. *Nat. Rev. Neurosci.* 19, 701–710. <https://doi.org/10.1038/s41583-018-0068-2>.
- Campanozano, V., Montermini, L., Moltó, M.D., Pianese, L., Cossée, M., Cavalcanti, F., Monros, E., Rodius, F., Duclos, F., Monticelli, A., Zara, F., Cañizares, J., Koutnikova, H., Bidichandani, S.I., Gellera, C., Brice, A., Trouillas, P., De Michele, G., Filla, A., De Frutos, R., Palau, F., Patel, P.I., Di Donato, S., Mandel, J.L., Coccoza, S., Koenig, M., Pandolfo, M., 1996. Friedreich's ataxia: autosomal recessive disease caused by an intronic GAA triplet repeat expansion. *Science* 271, 1423–1427. <https://doi.org/10.1126/science.271.5254.1423>.
- Coccoza, S., Costabile, T., Tedeschi, E., Abate, F., Russo, C., Liguori, A., Del Vecchio, W., Paciello, F., Quarantelli, M., Filla, A., Brunetti, A., Saccà, F., 2018. Cognitive and functional connectivity alterations in Friedreich's ataxia. *Ann. Clin. Transl. Neurol.* 5, 677–686. <https://doi.org/10.1002/acn3.555>.
- Dadsena, R., Wetz, S., Hofmann, A., Costa, A.S., Romanzetti, S., Lischewski, S.A., Krockauer, C., Balloff, C., Binkofski, F., Schulz, J.B., Reetz, K., Walders, J., 2025. Evidence of clinical and brain recovery in post-COVID-19 condition: a three-year follow-up study. *Brain Commun* fca366. <https://doi.org/10.1093/braincomms/fca366>.
- Della Nave, R., Ginestroni, A., Tessa, C., Salvatore, E., Bartolomei, I., Salvi, F., Dotti, M. T., De Michele, G., Piacentini, S., Mascalchi, M., 2008. Brain white matter tracts degeneration in Friedreich ataxia. An in vivo MRI study using tract-based spatial statistics and voxel-based morphometry. *NeuroImage* 40, 19–25. <https://doi.org/10.1016/j.neuroimage.2007.11.050>.
- Dogan, I., Romanzetti, S., Didszun, C., Mirzazade, S., Timmann, D., Saft, C., Schöls, L., Synofzik, M., Giordano, I.A., Klockgether, T., Schulz, J.B., Reetz, K., 2019. Structural characteristics of the central nervous system in Friedreich ataxia: an in vivo spinal cord and brain MRI study. *J. Neurol. Neurosurg. Psychiatry* 90, 615–617. <https://doi.org/10.1136/jnnp-2018-318422>.
- Dogan, I., Tinnemann, E., Romanzetti, S., Mirzazade, S., Costa, A.S., Werner, C.J., Heim, S., Fedosov, K., Schulz, S., Timmann, D., Giordano, I.A., Klockgether, T., Schulz, J.B., Reetz, K., 2016. Cognition in Friedreich's ataxia: a behavioral and multimodal imaging study. *Ann. Clin. Transl. Neurol.* 3, 572–587. <https://doi.org/10.1002/acn3.315>.
- Esteban, O., Birman, D., Schaer, M., Koyejo, O.O., Poldrack, R.A., Gorgolewski, K.J., 2017. MRIQC: advancing the automatic prediction of image quality in MRI from unseen sites. *PLoS ONE* 12, e0184661. <https://doi.org/10.1371/journal.pone.0184661>.
- Georgiou-Karistianis, N., Corben, L.A., Lock, E.F., Bujalka, H., Adanyeguh, I., Corti, M., Deelchand, D.K., Delatycki, M.B., Dogan, I., Farmer, J., França, M.C., Gabay, A.S., Gaetz, W., Harding, I.H., Joers, J., Lax, M.A., Li, J., Lynch, D.R., Mareci, T.H., Martinez, A.R.M., Pandolfo, M., Papoutsis, M., Parker, R.G., Reetz, K., Rezende, T.J.R., Roberts, T.P., Romanzetti, S., Rudko, D.A., Saha, S., Schulz, J.B., Subramony, S. H., Supramaniam, V.G., Lenglet, C., Henry, P.G., 2025. Neuroimaging biomarkers for Friedreich Ataxia: a cross-sectional analysis of the TRACK-FA study. *Ann. Neurol.* 98, 386–397. <https://doi.org/10.1002/ana.27237>.
- Ginestroni, A., Diciotti, S., Cecchi, P., Pesaresi, I., Tessa, C., Giannelli, M., Della Nave, R., Salvatore, E., Salvi, F., Dotti, M.T., Piacentini, S., Soricelli, A., Cosottini, M., De Stefano, N., Mascalchi, M., 2012. Neurodegeneration in Friedreich's ataxia is associated with a mixed activation pattern of the brain. A fMRI study. *Hum. Brain Mapp.* 33, 1780–1791. <https://doi.org/10.1002/hbm.21319>.
- Glickman, M.E., Rao, S.R., Schultz, M.R., 2014. False discovery rate control is a recommended alternative to Bonferroni-type adjustments in health studies. *J. Clin. Epidemiol.* 67, 850–857. <https://doi.org/10.1016/j.jclinepi.2014.03.012>.
- Gronwall, D.M., 1977. Paced auditory serial-addition task: a measure of recovery from concussion. *Percept. Mot. Skills* 44, 367–373. <https://doi.org/10.2466/pms.1977.44.2.367>.
- Han, Y., Wang, J., Zhao, Z., Min, B., Lu, J., Li, K., He, Y., Jia, J., 2011. Frequency-dependent changes in the amplitude of low-frequency fluctuations in amnesic mild cognitive impairment: a resting-state fMRI study. *NeuroImage* 55, 287–295. <https://doi.org/10.1016/j.neuroimage.2010.11.059>.
- Harding, I.H., Chopra, S., Arrigoni, F., Boesch, S., Brunetti, A., Coccoza, S., Corben, L.A., Deistung, A., Delatycki, M., Diciotti, S., Dogan, I., Evangelisti, S., França, M.C., Góricke, S.L., Georgiou-Karistianis, N., Gramigna, L.L., Henry, P.G., Hernandez-Castillo, C.R., Hutter, D., Jahanshad, N., Joers, J.M., Lenglet, C., Lodi, R., Manners, D.N., Martinez, A.R.M., Martinuzzi, A., Marzi, C., Mascalchi, M., Nachbauer, W., Pane, C., Peruzzo, D., Pisharady, P.K., Pontillo, G., Reetz, K., Rezende, T.J.R., Romanzetti, S., Saccà, F., Scherfler, C., Schulz, J.B., Stefani, A., Testa, C., Thomopoulos, S.I., Timmann, D., Tirelli, S., Tonon, C., Vavla, M., Egan, G. F., Thompson, P.M., 2021a. Brain structure and degeneration staging in Friedreich Ataxia: magnetic resonance imaging volumetrics from the ENIGMA-Ataxia working group. *Ann. Neurol.* 90, 570–583. <https://doi.org/10.1002/ana.26200>.
- Harding, I.H., Corben, L.A., Delatycki, M.B., Stagnitti, M.R., Storey, E., Egan, G.F., Georgiou-Karistianis, N., 2017. Cerebral compensation during motor function in Friedreich ataxia: the IMAGE-FRDA study. *Mov. Disord. Off. J. Mov. Disord. Soc.* 32, 1221–1229. <https://doi.org/10.1002/mds.27023>.
- Harding, I.H., Corben, L.A., Storey, E., Egan, G.F., Stagnitti, M.R., Poudel, G.R., Delatycki, M.B., Georgiou-Karistianis, N., 2015. Fronto-cerebellar dysfunction and dysconnectivity underlying cognition in Friedreich ataxia: the IMAGE-FRDA study. *Hum. Brain Mapp.* 37, 338–350. <https://doi.org/10.1002/hbm.23034>.
- Henschel, L., Conjeti, S., Estrada, S., Diers, K., Fischl, B., Reuter, M., 2020. FastSurfer - A fast and accurate deep learning based neuroimaging pipeline. *NeuroImage* 219, 117012. <https://doi.org/10.1016/j.neuroimage.2020.117012>.
- Henschel, L., Kügler, D., Reuter, M., 2022. FastSurferV1NN: building resolution-independence into deep learning segmentation methods—a solution for HighRes brain MRI. *NeuroImage* 251, 118933. <https://doi.org/10.1016/j.neuroimage.2022.118933>.
- Hohenfeld, C., Werner, C.J., Reetz, K., 2018. Resting-state connectivity in neurodegenerative disorders: is there potential for an imaging biomarker? *NeuroImage Clin* 18, 849–870. <https://doi.org/10.1016/j.nicl.2018.03.013>.
- Jacobi, H., Rakowicz, M., Rola, R., Fancellu, R., Mariotti, C., Charles, P., Durr, A., Küper, M., Timmann, D., Linnemann, C., Schöls, L., Kaut, O., Schaub, C., Filla, A., Baliko, L., Melegh, B., Kang, J.S., Giunti, P., Warrenburg, B., Klockgether, T., 2012. Inventory of non-ataxia signs (INAS): validation of a new clinical assessment instrument. *Cerebellum Lond. Engl* 12. <https://doi.org/10.1007/s12311-012-0421-3>.
- Jia, X.Z., Sun, J.W., Ji, G.J., Liao, W., Lv, Y.T., Wang, J., Wang, Z., Zhang, H., Liu, D.Q., Zang, Y.F., 2020. Percent amplitude of fluctuation: a simple measure for resting-state fMRI signal at single voxel level. *PLOS ONE* 15, e0227021. <https://doi.org/10.1371/journal.pone.0227021>.
- Jing, Y., Dogan, I., Dadsena, R., Faber, J., Schulz, J.B., Reetz, K., Romanzetti, S., 2025. Multimodal imaging investigation of the Dentato-Thalamo-Cortical pathway in Friedreich's Ataxia. *Mov. Disord.* <https://doi.org/10.1002/mds.70179>.
- Kerestes, R., Cummins, H., Georgiou-Karistianis, N., Selvadurai, L.P., Corben, L.A., Delatycki, M.B., Egan, G.F., Harding, I.H., 2023. Reduced cerebello-cerebral functional connectivity correlates with disease severity and impaired white matter integrity in Friedreich ataxia. *J. Neurol.* 270, 2360–2369. <https://doi.org/10.1007/s00415-023-11637-x>.
- Koeppe, A.H., Mazurkiewicz, J.E., 2013. Friedreich ataxia: neuropathology revised. *J. Neuropathol. Exp. Neurol.* 72, 78–90. <https://doi.org/10.1097/NEN.0b013e31827e5762>.
- Nasreddine, Z.S., Phillips, N.A., Bédirian, V., Charbonneau, S., Whitehead, V., Collin, I., Cummings, J.L., Chertkow, H., 2005. The Montreal Cognitive Assessment, MoCA: a brief screening tool for mild cognitive impairment. *J. Am. Geriatr. Soc.* 53, 695–699. <https://doi.org/10.1111/j.1532-5415.2005.53221.x>.
- Niemann, H., Sturm, W., Thöne-Otto, A.L.T., Willmes, K., 2008. CVLT California verbal learning test. German adaptation. Manual.

- Nieto-Castanon, A., 2020. Handbook of functional connectivity magnetic resonance imaging methods in CONN. <https://doi.org/10.56441/hilbertpress.2207.6598>.
- Nieto-Castanon, A., Whitfield-Gabrieli, S., 2022. CONN functional connectivity toolbox: RRID SCR_009550, release 22. <https://doi.org/10.56441/hilbertpress.2246.5840>.
- Parkes, L., Fulcher, B., Yücel, M., Fornito, A., 2018. An evaluation of the efficacy, reliability, and sensitivity of motion correction strategies for resting-state functional MRI. *NeuroImage* 171, 415–436. <https://doi.org/10.1016/j.neuroimage.2017.12.073>.
- Reetz, K., Dogan, I., Costa, A.S., Dafotakis, M., Fedosov, K., Giunti, P., Parkinson, M.H., Sweeney, M.G., Mariotti, C., Panzeri, M., Nanetti, L., Arpa, J., Sanz-Gallego, I., Durr, A., Charles, P., Boesch, S., Nachbauer, W., Klopstock, T., Karin, I., Depondt, C., Vom Hagen, J.M., Schöls, L., Giordano, I.A., Klockgether, T., Bürk, K., Pandolfo, M., Schulz, J.B., 2015. Biological and clinical characteristics of the European Friedreich's ataxia consortium for translational studies (EFACTS) cohort: a cross-sectional analysis of baseline data. *Lancet Neurol* 14, 174–182. [https://doi.org/10.1016/S1474-4422\(14\)70321-7](https://doi.org/10.1016/S1474-4422(14)70321-7).
- Reetz, K., Dogan, I., Hilgers, R.D., Giunti, P., Mariotti, C., Durr, A., Boesch, S., Klopstock, T., De Rivera, F.J.R., Schöls, L., Klockgether, T., Bürk, K., Rai, M., Pandolfo, M., Schulz, J.B., Nachbauer, W., Eigentler, A., Depondt, C., Benaich, S., Charles, P., Ewencyk, C., Monin, M.L., Dafotakis, M., Fedosov, K., Didszun, C., Ermis, U., Giordano, I.A., Timmann, D., Karin, I., Neuhofer, C., Stendel, C., Müller Vom Hagen, J., Wolf, J., Panzeri, M., Nanetti, L., Castaldo, A., Arpa, J., Sanz-Gallego, I., Parkinson, M.H., Sweeney, M.G., 2016. Progression characteristics of the European friedreich's ataxia consortium for translational studies (EFACTS): a 2 year cohort study. *Lancet Neurol* 15, 1346–1354. [https://doi.org/10.1016/S1474-4422\(16\)30287-3](https://doi.org/10.1016/S1474-4422(16)30287-3).
- Reetz, K., Dogan, I., Hilgers, R.D., Giunti, P., Parkinson, M.H., Mariotti, C., Nanetti, L., Durr, A., Ewencyk, C., Boesch, S., Nachbauer, W., Klopstock, T., Stendel, C., Rodríguez De Rivera Garrido, F.J., Rummey, C., Schöls, L., Hayer, S.N., Klockgether, T., Giordano, I., Didszun, C., Rai, M., Pandolfo, M., Schulz, J.B., Labrum, R., Thomas-Black, G., Manso, K., Solanky, N., Geller, C., Mongelli, A., Castaldo, A., Fichera, M., 2021. Progression characteristics of the European Friedreich's Ataxia Consortium for Translational Studies (EFACTS): a 4-year cohort study. *Lancet Neurol* 20, 362–372. [https://doi.org/10.1016/S1474-4422\(21\)00027-2](https://doi.org/10.1016/S1474-4422(21)00027-2).
- Reetz, K., Dogan, I., Hohenfeld, C., others, 2018. Nonataxia symptoms in Friedreich ataxia: report from the registry of the European Friedreich's ataxia consortium for translational studies (EFACTS). *Neurology* 91, e917–e930.
- Reetz, K., Lischewski, S.A., Dogan, I., Didszun, C., Pishnamaz, M., Konrad, K., Marx-Schütt, K., Farmer, J., Lynch, D.R., Corben, L.A., Pandolfo, M., Schulz, J.B., Costa, A. S., Romanzetti, S., Dadsena, R., Praster, M., Clavel, T., Jankowski, V., Jankowski, J., Pabst, O., Marx, N., Möllmann, J., Jacobsen, M., Dukart, J., Eickhoff, S., Hilgers, R. D., 2025. Friedreich's ataxia—A rare multisystem disease. *Lancet Neurol* 24, 614–624. [https://doi.org/10.1016/S1474-4422\(25\)00175-9](https://doi.org/10.1016/S1474-4422(25)00175-9).
- Rezende, T.J.R., Adanyeguh, I.M., Arrigoni, F., Bender, B., Cendes, F., Corben, L.A., Deistung, A., Delatycki, M., Dogan, I., Egan, G.F., Göricke, S.L., Georgiou-Karistianis, N., Henry, P.G., Hutter, D., Jahanshad, N., Joers, J.M., Lenglet, C., Lindig, T., Martinez, A.R.M., Martinuzzi, A., Paparella, G., Peruzzo, D., Reetz, K., Romanzetti, S., Schöls, L., Schulz, J.B., Synofzik, M., Thomopoulos, S.I., Thompson, P.M., Timmann, D., Harding, I.H., França Jr, M.C., 2023. Progressive spinal cord degeneration in Friedreich's Ataxia: results from ENIGMA-Ataxia. *Mov. Disord.* 38, 45–56. <https://doi.org/10.1002/mds.29261>.
- Rubin, R.D., Watson, P.D., Duff, M.C., Cohen, N.J., 2014. The role of the hippocampus in flexible cognition and social behavior. *Front. Hum. Neurosci.* 8. <https://doi.org/10.3389/fnhum.2014.00742>.
- Schmahmann, J.D., Sherman, J.C., 1998. The cerebellar cognitive affective syndrome. *Brain J. Neurol.* 121 (Pt 4), 561–579. <https://doi.org/10.1093/brain/121.4.561>.
- Schmitz-Hübsch, T., Du Montcel, S.T., Baliko, L., Berciano, J., Boesch, S., Depondt, C., Klockgether, T., 2006. Scale for the assessment and rating of ataxia: development of a new clinical scale. *Neurology* 66, 1717–1720.
- Schmitz-Hübsch, T., Giunti, P., Stephenson, D.A., Globas, C., Baliko, L., Saccà, F., Mariotti, C., Rakowicz, M., Szymanski, S., Infante, J., van de Warrenburg, B.P.C., Timmann, D., Fancellu, R., Rola, R., Depondt, C., Schöls, L., Zdzienicka, E., Kang, J. S., Döhlinger, S., Kremer, B., Melegh, B., Filla, A., Klockgether, T., 2008. SCA Functional Index: a useful compound performance measure for spinocerebellar ataxia. *Neurology* 71, 486–492. <https://doi.org/10.1212/01.wnl.0000324863.76290.19>.
- Selvadurai, L.P., Corben, L.A., Delatycki, M.B., Storey, E., Egan, G.F., Georgiou-Karistianis, N., Harding, I.H., 2020. Multiple mechanisms underpin cerebral and cerebellar white matter deficits in Friedreich ataxia: the IMAGE-FRDA study. *Hum. Brain Mapp.* 41, 1920–1933. <https://doi.org/10.1002/hbm.24921>.
- Selvadurai, L.P., Georgiou-Karistianis, N., Shishegar, R., Sheridan, C., Egan, G.F., Delatycki, M.B., Harding, I.H., Corben, L.A., 2021. Longitudinal structural brain changes in Friedreich ataxia depend on disease severity: the IMAGE-FRDA study. *J. Neurol.* 268, 4178–4189. <https://doi.org/10.1007/s00415-021-10512-x>.
- Strauss, E., Sherman, E.M.S., Spreen, O., 2006. *A Compendium of Neuropsychological Tests: Administration, Norms, And Commentary, 3rd ed, A Compendium of Neuropsychological Tests: Administration, Norms, And Commentary, 3rd ed.* Oxford University Press, New York, NY, US.
- Tranfa, M., Costabile, T., Pontillo, G., Scaravilli, A., Pane, C., Brunetti, A., Saccà, F., Cocozza, S., 2025. Altered intracerebellar functional connectivity in Friedreich's ataxia: a graph-theory functional MRI study. *The Cerebellum* 24, 30. <https://doi.org/10.1007/s12311-025-01785-3>.
- Vavla, M., Arrigoni, F., Peruzzo, D., Montanaro, D., Frijia, F., Pizzighello, S., De Luca, A., Della Libera, E., Tessarotto, F., Guerra, P., Harding, I.H., Martinuzzi, A., 2022. Functional MRI studies in Friedreich's Ataxia: a systematic review. *Front. Neurol.* 12, 802496. <https://doi.org/10.3389/fneur.2021.802496>.
- Yang, H., Long, X.Y., Yang, Y., Yan, H., Zhu, C.Z., Zhou, X.P., Zang, Y.F., Gong, Q.Y., 2007. Amplitude of low frequency fluctuation within visual areas revealed by resting-state functional MRI. *NeuroImage* 36, 144–152. <https://doi.org/10.1016/j.neuroimage.2007.01.054>.
- Yang, L., Yan, Y., Wang, Y., Hu, X., Lu, J., Chan, P., Yan, T., Han, Y., 2018. Gradual disturbances of the amplitude of low-frequency fluctuations (ALFF) and fractional ALFF in Alzheimer spectrum. *Front. Neurosci.* 12. <https://doi.org/10.3389/fnins.2018.00975>.
- Zou, Q.H., Zhu, C.Z., Yang, Y., Zuo, X.N., Long, X.Y., Cao, Q.J., Wang, Y.F., Zang, Y.F., 2008. An improved approach to detection of amplitude of low-frequency fluctuation (ALFF) for resting-state fMRI: fractional ALFF. *J. Neurosci. Methods* 172, 137–141. <https://doi.org/10.1016/j.jneumeth.2008.04.012>.